LANGMUIR

pubs.acs.org/Langmuir Article

Construction of Low-Energy Prepared Highly Stable Surfactant Emulsion by Optimizing Composition Configuration

Fang Wang, Cheng Ma,* and Jianbin Huang*

Cite This: *Langmuir* 2025, 41, 14570−14578 Read Online

ACCESS | Metrics & More | Article Recommendations | Supporting Information

ABSTRACT: Emulsion systems that are independent of preparation conditions and time are ideal models for fundamental emulsion research. However, special strategies are required to form these emulsions, particularly with commonly used oils and emulsifiers that have proven to be more difficult. In this study, an efficient approach to preparing a low-energy emulsion with outstanding stability is reported. This approach is derived from a comprehensive study of the component composition in the residual emulsified fractions in water-separation emulsions. The outstandingly stable emulsion exhibits a highly stacked droplet structure, which can restrict the droplet movement within the disperse medium, accompanied by a stable oil−water interface layer, which can hinder the molecular exchange between droplets and resist droplet destruction under extreme conditions, thereby preventing the demulsification caused by sedimentation, coalescence, and Ostwald ripening. These peculiarities enable the emulsion to remain stable over long periods and at elevated temperatures, even exhibiting a spontaneous tendency to recover to the emulsion after centrifugal phase splitting. This approach lends itself to generalization in the context of multiple surfactants or oil phases, thus establishing a foundation for the study of various emulsifiers and functional emulsions. Moreover, the low-energy-input preparation can reduce energy consumption in the emulsion production, aligning with the principles of green development.

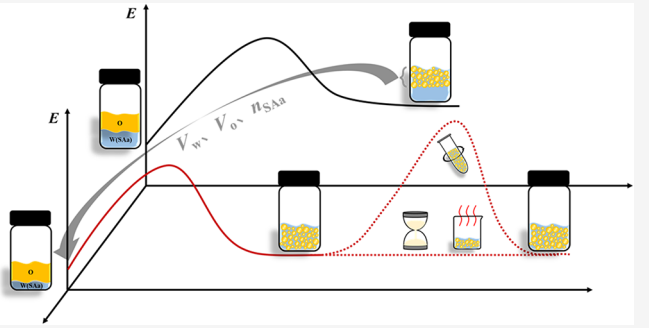

INTRODUCTION

The stable dispersion of oil in aqueous media represents a fundamental scientific problem that is of great consequence to a number of processes,[1,2] including drug delivery,[3] interfacial catalysis,[4] and rheology modulation.[5] Due to the high internal phase capacity and economical preparation, the oil−water emulsions have attracted significant attention in a number of important applications, such as pharmaceuticals,[6] pesticides,[7] chemicals,[8] food,[9] and petroleum extraction.[10,11] However, the emulsion structure and properties are dependent on the preparation conditions and placement time,[12,13] which presents a challenge in ensuring the repeatability of sample observation and characterization. This has hindered fundamental scientific research on emulsions, including understanding the constitutive law and stabilization mechanism, and has severely limited the development of emulsion applications. Therefore, the development of highly stable emulsions by low-energy preparation has emerged as a pivotal research focus.

Although the development of systems such as Pickering emulsions stabilized by nanoparticles coexisting with surfactants has led to breakthroughs in improving emulsion stability,[14,15] these systems still have limitations in terms of low-energy preparation.[16,17] Nowadays, surfactant emulsions are the preferred option for industrial applications. From the perspective of preparation, surfactant small molecules are capable of spontaneously dissolving and diffusing into the oil/water interface in oil−water systems, thereby eliminating the need for additional energy consumption in the emulsification process. Furthermore, surfactant emulsions with a high internal phase content (φ > 74%, i.e., high internal phase emulsion, HIPE) can be applied without reverse rotation.[18] Consequently, the current research should focus on the high stability of the surfactant emulsion, based on its low-energy preparation and high internal phase content.

N-Hexadecane (the largest liquid alkane at room temperature) is an important constituent of mineral oils and is also frequently utilized in various studies of oil−water dispersion systems.[19] Beattie and Djerdjev employed hexadecane as a model oil phase to study the stabilization mechanism of oil droplets in water.[20] Tcholakova et al. investigated the effect of different surfactants on the stability of hexadecane/water emulsion systems.[21] Hence, hexadecane was selected as the ideal oil phase in this work. Meanwhile, typical surfactants such as sodium dodecyl sulfate (SDS) and dodecyl trimethylammo-

Received: April 18, 2025
Revised: May 15, 2025
Accepted: May 15, 2025
Published: May 23, 2025

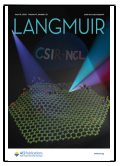

https://doi.org/10.1021/acs.langmuir.5c01936
Langmuir 2025, 41, 14570−14578

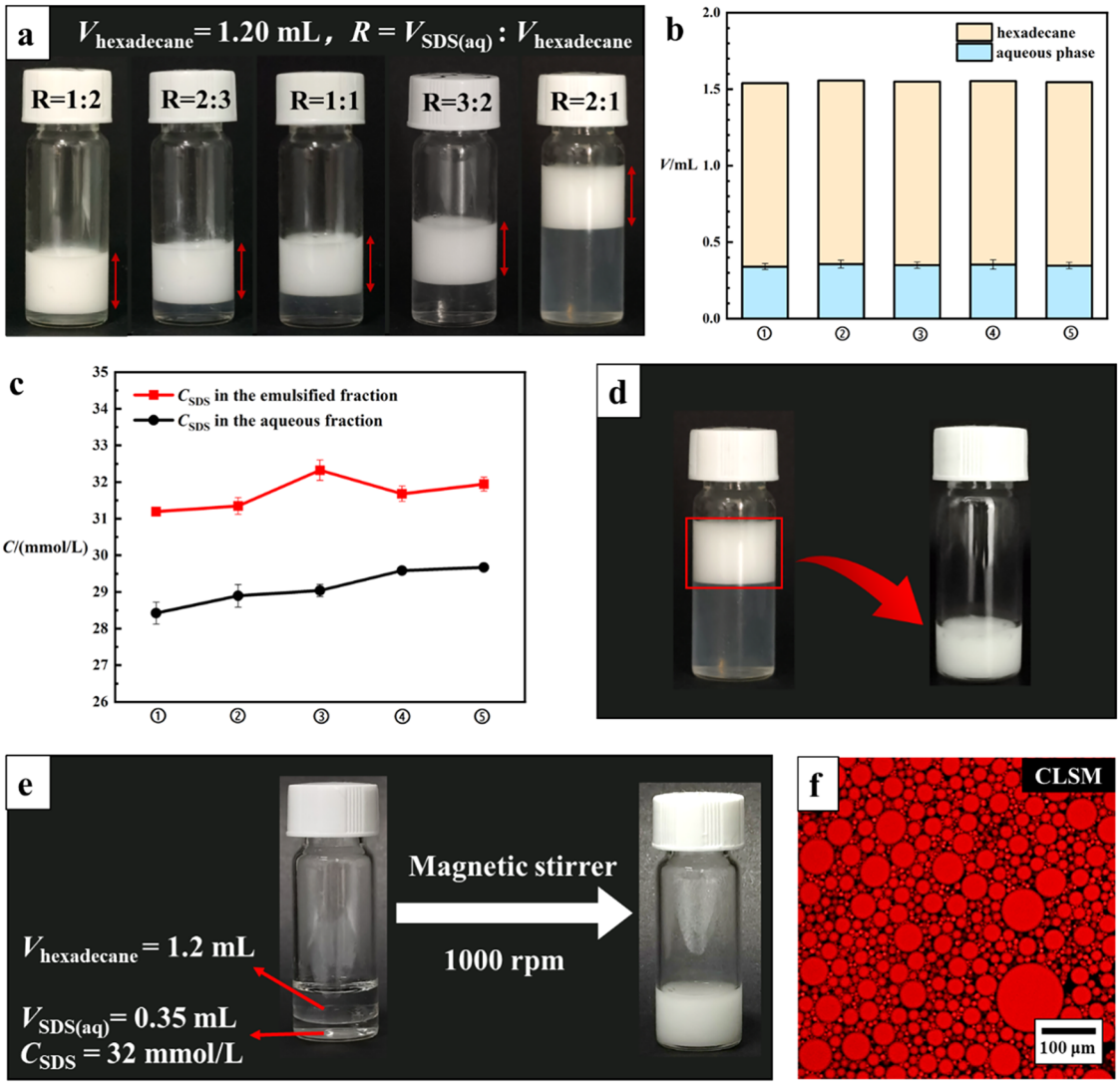

Figure 1. (a) Macrographs of emulsions prepared with $V_{SDS(aq)}/V_{hexadecane}$ as 1:2, 2:3, 1:1, 3:2, and 2:1, respectively ($V_{hexadecane}$ = 1.20 mL, $C_{SDS(aq)}$ = 30 mmol/L). (b) Volumes of hexadecane and aqueous phase in the emulsified fractions of five samples (sample numbers ①, ②, ③, ④, and ⑤ refer to emulsions prepared with $V_{SDS(aq)}/V_{hexadecane}$ as 1:2, 2:3, 1:1, 3:2, and 2:1, respectively). (c) SDS concentrations in the emulsified fractions and aqueous fractions of five samples (sample numbers ①, ②, ③, ④, and ⑤ refer to emulsions prepared with $V_{SDS(aq)}/V_{hexadecane}$ as 1:2, 2:3, 1:1, 3:2, and 2:1, respectively). (d) Macroscopic state of the emulsified fraction was isolated and observed. (e) Stable emulsion was produced by configuring the emulsion according to the analyzed stoichiometric ratios. (f) Micrographs of the produced emulsion by CLSM.

nium chloride (DTAC) were chosen as emulsifiers. The low-energy preparation was conducted using magnetic stirring at 1000 rpm, in comparison to high-energy preparations of O/W emulsions with other emulsifiers, such as ultrasonic (240 W),[22] high-speed stirring (>10,000 rpm),[23] or the high-pressure homogenizing (30 MPa)[24] (a detailed comparison is shown in Table S1). In order to ascertain the emulsion stability, both the macro- and microscale retentions were considered the defining criteria. In addition to the aging test, the stability of emulsions was also analyzed under extreme conditions, including heating and centrifugation.

Here, a general approach to constructing outstandingly stable surfactant emulsions by low-energy preparation is investigated. The emulsions are constituted solely of oil, water, and a minor concentration of surfactant. Various surfactant emulsions were fabricated and studied by visual observation, component analysis, and microstructural characterization. The stability mechanism of emulsions was explored by analyzing the deformation and motion behaviors of emulsion droplets under different conditions, utilizing a combination of staining processing, transmission electron microscopy, and heat stage microscopy.

EXPERIMENTAL SECTION

Materials. The sodium dodecyl sulfate (SDS) (99%, AR) was purchased from Aladdin. The hexadecane (99%, AR), decane (98%, AR), and sodium laurate (98%, AR) were purchased from Energy Chemical. The diethylbenzene (98%, RG) was purchased from Adamas. The ethyl caprate (99%, AR) was purchased from C. The mineral oil (CP) was purchased from Shanghai Yuanye Biotechnology. The dodecyl trimethylammonium chloride (99%, LR) and primary alcohol ethoxylate 7 (LR) were products from Shanghai Dibai Biotechnology. The Oil Red O (biological stain) was purchased from Beijing Xinxiyuan Biotechnology. The Nile Red (98%, LC) was purchased from Beijing Konoscience Technology. Aqueous solutions were prepared using Milli-Q water of ~18.3 MΩ·cm.

Emulsion Preparation. Precalculated surfactant powder was weighed and then dissolved in Milli-Q water at room temperature. Following this, oil was added to the surfactant aqueous solution with

https://doi.org/10.1021/acs.langmuir.5c01936
Langmuir 2025, 41, 14570−14578

precalculated volumes, resulting in a biphasic liquid with water−oil stratification. Emulsification of the biphasic liquid was performed at room temperature at 1000 rpm (5 gear) for 30 min using a magnetic stirrer (C-MAG HS7, IKA, Germany). All of the emulsions were stored at room temperature before further characterization.

Emulsion Analysis. The volume of water in the emulsion part was calculated as the added water volume minus the dropout water volume. The volume of oil in the emulsion part was the volume of added oil by default. The surfactant amount in the emulsion part was calculated as the added surfactant amount minus the surfactant amount in the dropout water, while the surfactant amount in the dropout water was measured by a two-phase titration method.[25] The surfactant aqueous solutions with concentrations of 0.1, 0.5, 1, 1.5, and 2 mmol/L were first measured to draw a standard curve. Ten milliliters of the surfactant aqueous solution and 5 mL of trichloromethane were mixed. Then, a small amount of Dimidium Bromide-Acid blue mixed indicator was added, making the organic layer pink. Benzylonium chloride standard solution (0.004009 mol/L) was used to titrate the surfactant solution. When the organic layer changed from pink to blue, the titration ended, and the volume of the used standard solution was recorded. With the dropout water diluted and titrated, the surfactant concentration in the dropout water was calculated according to the standard curve.

Emulsion Characterizations. The appearance of emulsions was observed by a digital camera. The microscopic structure of the emulsions was observed by optical microscopy (OM) and confocal laser scan microscopy (CLSM). In the OM measurements, the emulsion sample was put on a glass plate with a cover glass and observed by optical microscopy (BX51, Olympus, Japan). The digital video was transferred to a computer through a video capture board and was recorded into JPG images using the software. In the CLSM measurements, the oil phase was stained with Nile Red (red fluorescent). A drop (about 10 μL) of the stained emulsion sample was sealed between two slides, ready for CLSM observation. A TCS-sp inverted confocal laser scanning microscope (Leica, Germany) was used to conduct experiments in the florescence and differential interference contrast (DIC) modes. Laser scanning confocal images were performed on a Nikon A1R Si microscope. The droplet size of emulsions was measured using a Mastersizer (Malven Instruments Ltd., Malvern, U.K.). In order to ensure that the optical density during the measurement process is between 10 and 20%, the 0.5 mL emulsion sample was added to 800 mL of deionized water; after being diluted homogeneously, the droplet size distribution was measured, and then the average droplet size and uniformity were calculated.

Emulsion Stability. The emulsion stability was evaluated by different tests. An aging test was performed by storing the emulsion in a biochemical incubator (SPX-263, Ningbo Jiangnan Instrument Factory, China) at a constant temperature of 25 °C for up to 12 months. High-temperature test was evaluated at 50 °C and 90 °C within an electric thermostatic dryer (DH-202, Tianjin Zhonghuan Furnace Corp, China) for 12 h. The resistance to centrifugal force was tested by centrifugation at 8000 rpm for 10 min using a centrifuge tube (MG1650, Merrick Instruments (Shanghai) Co. Ltd., China), and repeating the cycles 3 times and prolonging the time to 30 min.

Droplet Behavior Observation with Staining Processing. In comparison with unstained emulsions, the stained emulsions were prepared with the oil phase stained by Oil Red O. The stained and unstained emulsions were contacted without any disturbance for observing the droplet behaviors macroscopically. The stained and unstained emulsions were mixed by stirring for observing the droplet behaviors microscopically.

Droplet Position Observation under Heating Conditions. The emulsion droplet position under heating conditions was observed using a polar microscope with a heat stage (LV100N, Nikon, Japan). With the heat stage temperature set as 90 °C, the emulsion sample on a glass plate through a cover glass was placed and sealed in the heat stage. The droplet position was observed and recorded at the original state for 30 and 60 min. The droplet movement was analyzed according to the position variation.

TEM Observation. The structure of upper gelatinoid and bottom water split instantly after centrifugation was examined utilizing transmission electron microscopy (TEM) (FEI Tecnai G2 T20, 120 kV, together with energy-dispersive spectroscopy measurement). The samples were deposited onto copper grids of 230 mesh that were coated with Formvar film, and any additional liquid was wiped away using filter paper. The samples were left to dry at room temperature in preparation for TEM analysis.

RESULTS AND DISCUSSION

Construction of the Low-Energy Prepared Outstandingly Stable Emulsion (LEPOSE). With the fixed hexadecane volume ($V_{hexadecane}$) being 1.20 mL and the volume ratios of the SDS aqueous solution ($C_{SDS(aq)}$ as 30 mmol/L) to hexadecane ($V_{SDS(aq)}/V_{hexadecane}$) as 1:2, 2:3, 1:1, 3:2, 2:1, the 0.6 0.8, 1.2, 1.8, and 2.4 mL of SDS aqueous solution were added in five samples, respectively, and then the five samples were emulsified using low-energy magnetic stirring at 1000 rpm for 30 min. During the placement process at 25 °C, these prepared emulsions underwent rapid aqueous phase separation, yielding an aqueous fraction and an emulsified fraction. After a certain period of time, the volumes of the two fractions remained constant (Figure 1a).

Then, the composition analysis was conducted on these five samples, and the volumes of hexadecane and aqueous phase contained within the emulsified fractions of five samples were measured and are shown in Figure 1b, while the SDS concentrations (C_{SDS}) in emulsified fractions and aqueous fractions of five samples were measured and shown are in Figure 1c. It is worth noting that C_{SDS} in the emulsified fraction refers to the ratio of the SDS amount in the emulsified fraction to the volume of the aqueous phase in the emulsified fraction. As evidenced by the analyzed results, the component ratios in five emulsified fractions demonstrated consistency, where the C_{SDS} was found to be approximately 32 mmol/L and the $V_{aqueousphase}/V_{hexadecane}$ was found to be approximately 0.29. Subsequently, the macroscopic state of the emulsified fraction was isolated for observation, and it exhibited a stable macroscopic state (Figure 1d). This indicates that the emulsified fraction obtained from the water-separation emulsions is a highly stable emulsion.

Ingeniously, through configuring the hexadecane and SDS aqueous solution in accordance with the above-analyzed stoichiometric ratios, as illustrated in Figure 1e, with $V_{hexadecane}$ as 1.2 mL, $V_{SDS(aq)}$ as 0.35 mL, and $C_{SDS(aq)}$ as 32 mmol/L, a stable emulsion that did not separate oil or water was produced by low-energy magnetic stirring at 1000 rpm for 30 min. This finding underscores the correlation between the highly stable emulsion and water-separation emulsions. Furthermore, within the error ranges of the preparation conditions, the stable emulsion could be successfully prepared, with the macroscopic and microscopic morphology of the emulsion remaining relatively stable (Table S2), which allows for a certain margin of error in practical experimental operation.

The microstructure of the emulsion was revealed by confocal laser microscopy (CLSM). The emulsion was stained in the oil phase with Nile Red (red fluorescent). A large number of oil droplets in red fluorescence were observed, indicating an O/W structure of the emulsion (Figure 1f). With the critical micelle concentration (cmc) of the SDS as 8 mmol/L,[26] the SDS concentration in the emulsion is 4 cmc. With the interfacial tension between hexadecane and pure water at 37.5 mN/m,

https://doi.org/10.1021/acs.langmuir.5c01936
Langmuir 2025, 41, 14570−14578

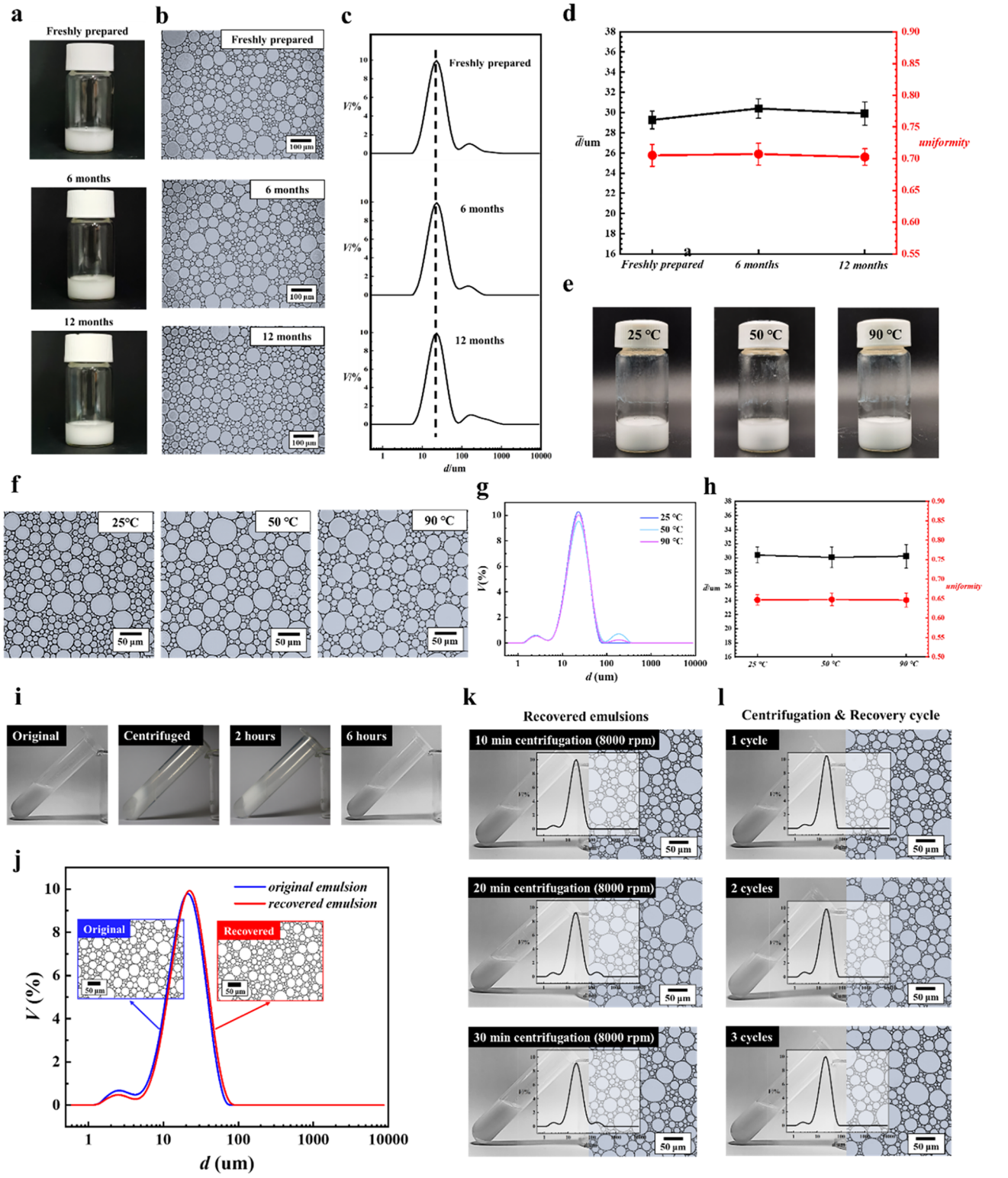

Figure 2. (a) Macrographs of the emulsion after different storage times (freshly prepared, 6 months, and 12 months). (b) Micrographs of the emulsion after different storage times (freshly prepared, 6 months, and 12 months). (c) Droplet size distribution of the emulsion after different storage times (freshly prepared, 6 months, and 12 months). (d) Trends of the average droplet diameter and the uniformity of the emulsion with storage time. (e) Macrographs of emulsion after placing at 25, 50, and 90 °C for 12 h. (f) Micrographs of emulsion after placing at 25, 50, and 90 °C for 12 h. (g) Droplet size distribution of emulsion after placing at 25, 50, and 90 °C for 12 h. (h) Trends of the average droplet diameter and the uniformity of emulsion with temperature. (i) Macrographs of the emulsion: original, instantly centrifuged, standing 2 h, standing 6 h (centrifugation at 8000 rpm for 10 min). (j) Micrographs and droplet size distribution of the original emulsion and recovered emulsion. (k) Macrographs, micrographs, and droplet size distribution of recovered emulsions: centrifugation at 8000 rpm for 10, 20, and 30 min. (l) Macrographs, micrographs, and droplet size distribution of recovered emulsions: centrifugation (at 8000 rpm for 10 min) and recovery for 1 cycle, 2 cycles, and 3 cycles.

https://doi.org/10.1021/acs.langmuir.5c01936
Langmuir 2025, 41, 14570−14578

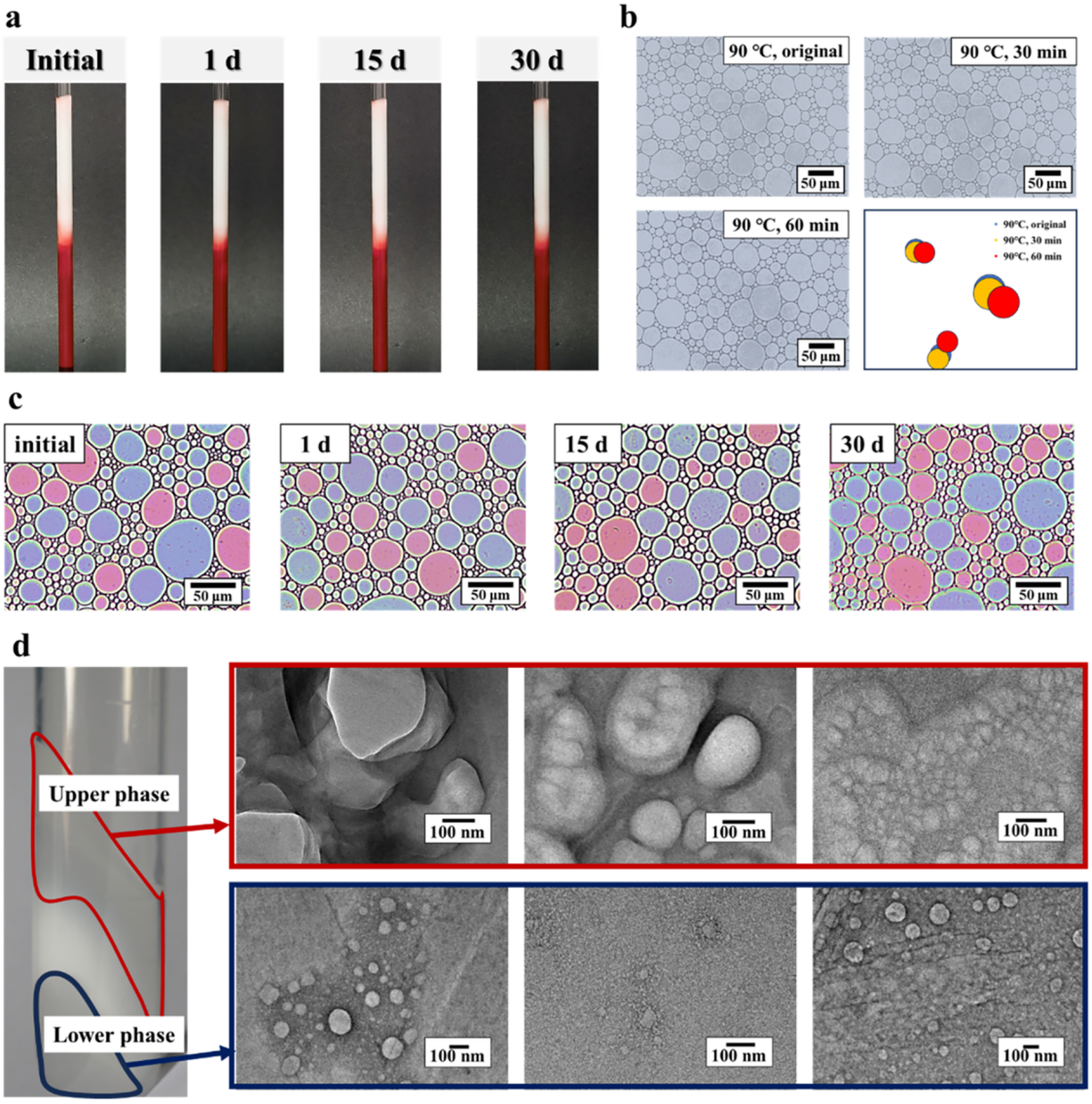

Figure 3. (a) Macrographs of contacted stained−unstained emulsion (initial, 1 day, 15 days, and 30 days). (b) Droplet position in the LEPOSE under 90 °C heating conditions (original, 30 min, and 60 min). (c) Micrographs of mixed stained−unstained emulsion (initial, 1 day, 15 days, and 30 days). (d) TEM photographs of the upper and lower phases in the instant phase splitting system after centrifugation.

the interfacial tension between hexadecane and SDS aqueous solution is 7.8 mN/m.

Stability of the LEPOSE. As demonstrated by aging tests at 25 °C, the emulsion exhibited outstanding stability, with its macroscopic morphology, microstructure, and droplet size distribution remaining consistent for a period of up to 12 months. Photographs of the emulsion samples after different storage times (freshly prepared, 6 months, and 12 months) are shown in Figure 2a. It can be observed that the emulsion remained fully emulsified within 12 months. Microscopic photographs also demonstrated that the microstructure of the emulsion remained in a state of crowded spherical droplets (Figure 2b). Furthermore, the droplet size distribution curves indicated that the droplet diameter remained within the range of 6−1000 μm over the 12-month period (Figure 2c). The trends of the average droplet diameter and the uniformity were calculated based on the droplet size distribution curves, demonstrating the year-long stability of the emulsion microstructure (Figure 2d).

In addition to the storage stability of emulsion under conventional conditions, the resistance of emulsion to high temperature and intense centrifugal field was also investigated, which is widely recognized to be extreme conditions that accelerate emulsion destruction and determine emulsion stability. It is generally believed that droplet movement is intensified at high temperatures, which increases the possibility of droplet collision and coalescence.[27] Therefore, the droplet usually appears to grow even during demulsification phenomena when the emulsion is heated. Distinctively, the emulsion in this study showed no change after being placed at higher temperatures of 50 and 90 °C for 12 h. The characteristic results of macromorphology (Figure 2e), micromorphology (Figure 2f), droplet size distribution (Figure 2g), and variation trends of the average droplet diameter and the uniformity (Figure 2h) of emulsion indicated that both emulsion appearance and microstructure did not change significantly under high-temperature conditions, which can be comparable to the thermostability of polymer emulsions[28] and Pickering emulsions.[29]

https://doi.org/10.1021/acs.langmuir.5c01936
Langmuir 2025, 41, 14570−14578

a

oil type	original	6 months	12 months	droplet size distribution
Decane	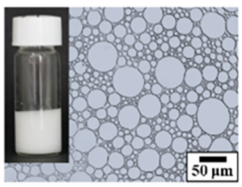	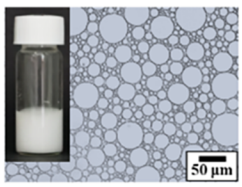	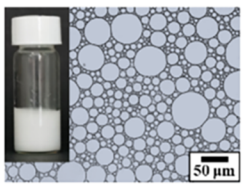	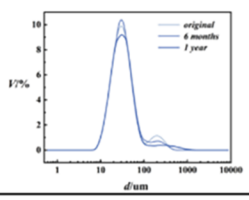
Diethylbenzene		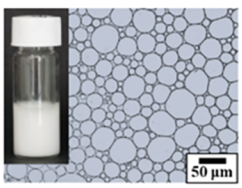	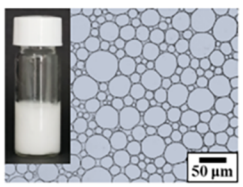	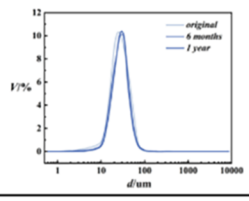
Ethyl caprate	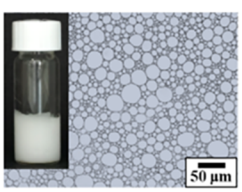	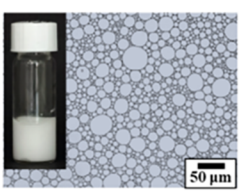	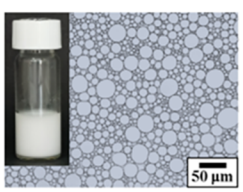	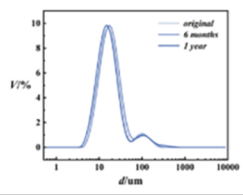
Mineral oil	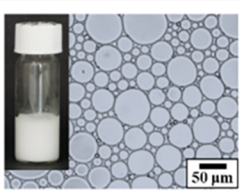	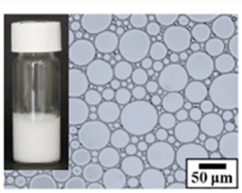	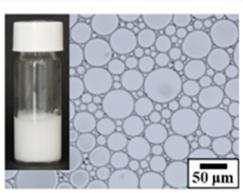	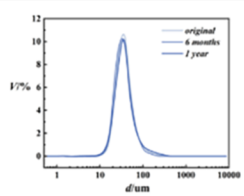

b

surfactant type	original	6 months	12 months	droplet size distribution
Sodium Laurate	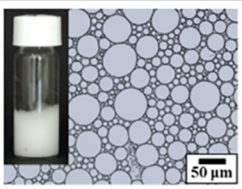	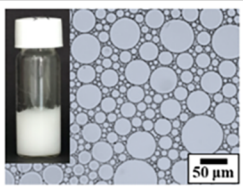	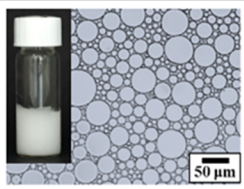	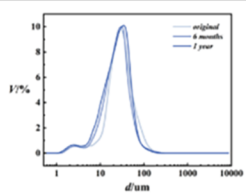
Dodecyl Trimethyl Ammonium Chloride	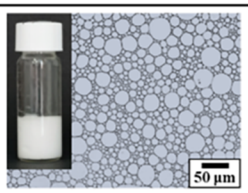	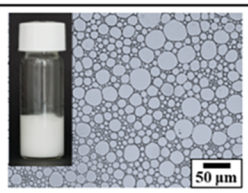	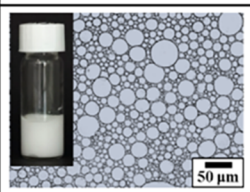	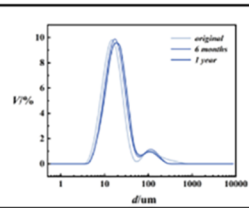
Primary Alcobol Ethoxylate 7	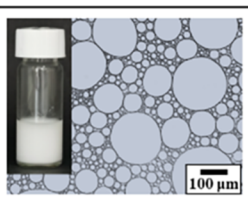	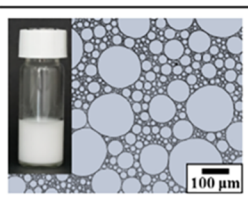	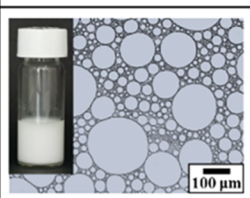	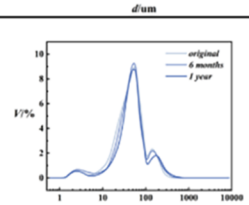

Figure 4. (a) Macrographs, micrographs, and droplet size distribution of emulsions prepared with various oils ($V_{oil}/V_{SDS(aq)}$ = 3.00, $C_{SDS(aq)}$ = 30 mmol/L (3.7 cmc)). (b) Macrographs, micrographs, and droplet size distribution of emulsions prepared with various surfactants ($V_{hexadecane}/V_{surfactant(aq)}$ = 3.00, $C_{sodiumlaurate(aq)}$ = 30 mmol/L (1 cmc), $C_{dodecyltrimethylammoniumchloride(aq)}$ = 30 mmol/L (1.6 cmc), $C_{primaryalcobolethoxylate7(aq)}$ = 30 mmol/L (600 cmc)).

https://doi.org/10.1021/acs.langmuir.5c01936
Langmuir 2025, 41, 14570−14578

High-speed centrifugation can greatly amplify the relative motion of the inner phase and the outer phase, thus intensifying the droplet coalescence.[30] Generally, the conditions for judging emulsion centrifugal stability are low speed (2000−4000 rpm) for a long time (30−60 min)[31] or high speed (6000−10,000 rpm) for a short time (10−20 min).[32] In this study, after centrifugation at 8000 rpm for 10 min, the emulsion showed phase splitting instantly; however, when the emulsion was left to stand at room temperature for 2 h, it was miraculously found that the emulsion fraction had increased markedly, further prolonging standing time to 6 h, the phase splitting phenomenon disappeared, and the emulsion completely recovered (Figure 2i). The microstructure and droplet size distribution curve of the recovered emulsion were consistent with those of the original emulsion (Figure 2j). This indicates that the emulsion has excellent self-recovery stability against centrifugal force, which suggests that the emulsion is in a thermodynamically mesostable state. To explore the ultimate conditions for centrifugal stability, the centrifugal time was increased to 20 and 30 min, and the emulsion can still recover (Figure 2k). Centrifugation and recovery cycle tests were conducted to investigate the fatigue resistance of the process. The results demonstrated that following three cycles, the emulsion exhibited the capacity to regain its original structural integrity (Figure 2l). The resistance to intense centrifugal field exhibited by the emulsion is comparable to that observed in polymer emulsions[33] and Pickering emulsions.[34]

Mechanism of the LEPOSE. The distinctive droplet structure of LEPOSE is a fundamental factor contributing to its exceptional stability, even under low-energy preparation conditions. In LEPOSE, the high degree of droplet stacking precludes the possibility of droplet movement, which would compound the laws of the Stockes sink-rate equation.[35] This allows for the maintenance of high stability, even at large droplet sizes. Observation of the stained and unstained LEPOSE over a period of one month showed that the emulsions of different colors remained distinct (Figure 3a). This finding suggests that despite the large droplet sizes, the droplets in LEPOSE exhibit minimal sedimentation, thereby maintaining a stable dispersion structure. Furthermore, this property also contributes to LEPOSE's stability to withstand elevated temperatures. As elevated temperatures can enhance the movement of emulsion droplets, the temperature was raised to a level that can disrupt the emulsion, whereas microscopic observation conducted at elevated temperatures revealed that the position of droplets in LEPOSE remained largely unchanged (Figure 3b).

It is also worth noting that the oil−water interface layer in LEPOSE plays an important role in determining its stability. The oil−water interface layer of LEPOSE impedes the exchange of oil molecules between disparate emulsion droplets. Following the stirring mixing of stained and unstained LEPOSE and the subsequent incubation for one month, it was found that the red and white emulsion droplets retained their distinct coloration under microscopic examination (Figure 3c). This observation suggests that the two emulsion droplets are not intermingled, suggesting that there is minimal internal molecular exchange. Following centrifugation, the oil−water interface layer was observed to retain its structural integrity, allowing the system to spontaneously recover to the emulsified state after phase splitting. The TEM photographs of the upper and lower phases in the instant phase splitting system after centrifugation are presented in Figure 3d. The lower phase shows the aqueous phase containing some droplet structures of 50−100 nm. It is postulated that these droplets are structures formed by the addition of solubilized hexadecane to the SDS micelles in the aqueous phase. There is an obvious network-like structure in the upper phase. Under the centrifugal field, the LEPOSE droplets only undergo deformation rather than coalescence, causing the oil−water interface layer and the external phase to be squeezed to form a network structure. During the standing process, this network structure can be reintegrated with the precipitated water to form an external phase again, which is manifested in the spontaneous recovery of the emulsion.

Generalization of the LEPOSE. In order to investigate the applicability of the LEPOSE construction approach in various emulsion application scenarios, a variety of oils and surfactants were employed to prepare LEPOSE. All of the emulsions displayed in Figure 4 were prepared by optimizing the composition configuration, in a manner analogous to that depicted in Figure 1e. Figure 4a shows the macromorphology and the microstructural analysis of emulsions prepared with different oils. A variety of oils, including alkanes, aromatic hydrocarbons, esters, and mineral oils, which are widely used in industry, could be used to construct LEPOSE by the same method. Similarly, LEPOSE can be obtained using other types of surfactants, including fatty acid-based surfactants, cationic surfactants, and nonionic surfactants (Figure 4b). As demonstrated in Figure 4, the low-energy formation and year-long stability can be achieved using various structures of oil and surfactants, verifying the generalizability of the LEPOSE construction approach. Thus, this emulsion construction approach has the potential to be applied in a variety of fields, such as pharmaceutical and chemical production. The oil−water interfacial tension of all emulsion systems in Figure 4 was measured and is shown in Figure S1.

CONCLUSIONS

A general approach to constructing a low-energy prepared outstandingly stable emulsion (LEPOSE) is presented based on a comprehensive study of the component composition in the residual emulsified fractions in water-separation emulsions. All of the LEPOSEs exhibit year-long stability in both macromorphology and microstructure. Furthermore, the LEPOSE demonstrates resistance to extreme conditions, including high temperature and an intense centrifugal field. Microscopic droplet behaviors were studied to explain the stability mechanism. The highly stacked droplet structure precludes the movement of droplets in the disperse medium, while the strength of the droplet interface layer prevents coalescence of droplets under extreme conditions, thereby ensuring the emulsion's outstanding stability.

A variety of oils and surfactants were employed in the preparation of LEPOSE, verifying the wide applicability of this approach. This finding not only facilitates the emulsion application but also provides an important model system for fundamental research on surfactant emulsion in terms of constitutive relationships and stability mechanisms. Furthermore, the low-energy consumption characteristics of emulsion preparation are consistent with the green development concept.

https://doi.org/10.1021/acs.langmuir.5c01936
Langmuir 2025, 41, 14570−14578

■ ASSOCIATED CONTENT

Supporting Information

The Supporting Information is available free of charge at https://pubs.acs.org/doi/10.1021/acs.langmuir.5c01936.

Emulsion preparation comparison; effects of preparation condition errors; and interfacial tension results (PDF)

■ AUTHOR INFORMATION

Corresponding Authors

Cheng Ma − *Beijing National Laboratory for Molecular Sciences (BNLMS), State Key Laboratory for Structural Chemistry of Unstable and Stable Species, College of Chemistry and Molecular Engineering, Peking University, Beijing 100871, China*; Email: 2406592570@pku.edu.cn

Jianbin Huang − *Beijing National Laboratory for Molecular Sciences (BNLMS), State Key Laboratory for Structural Chemistry of Unstable and Stable Species, College of Chemistry and Molecular Engineering, Peking University, Beijing 100871, China*; Email: jbhuang@pku.edu.cn

Author

Fang Wang − *Beijing National Laboratory for Molecular Sciences (BNLMS), State Key Laboratory for Structural Chemistry of Unstable and Stable Species, College of Chemistry and Molecular Engineering and School of Earth and Space Science, Peking University, Beijing 100871, China*; orcid.org/0009-0007-6348-4945

Complete contact information is available at: https://pubs.acs.org/10.1021/acs.langmuir.5c01936

Author Contributions

F.W.: methodology, formal analysis, investigation, resources, data curation, visualization, and writing the original draft. C.M.: methodology, resources, formal analysis, writing review and editing, and supervision. J.H.: conceptualization, writing review and editing, supervision, and funding acquisition.

Notes

The authors declare no competing financial interest.

■ ACKNOWLEDGMENTS

This work is supported by the National Natural Science Foundation of China (22272002).

■ REFERENCES

(1) Phipps, L. W. Mechanism of oil droplet fragmentation in high pressure homogenizers. *Nature* **1971**, *233*, 617−619.

(2) Anand, J. S.; Lal, D. Synthesis of methane from water for tritium measurement. *Nature* **1964**, *201*, 775−777.

(3) Gallarate, M.; Carlotti, M. E.; Trotta, M.; Bovo, S. On the stability of ascorbic acid in emulsified systems for topical and cosmetic use. *Int. J. Pharm.* **1999**, *188*, 233−241.

(4) Gong, J.; Bao, X. Fundamental insights into interfacial catalysis. *Chem. Soc. Rev.* **2017**, *46*, 1770−1771.

(5) Mason, T. G. New fundamental concepts in emulsion rheology. *Curr. Opin. Colloid Interface Sci.* **1999**, *4*, 231−238.

(6) Nikolic, I.; Mitsou, E.; Pantelic, I.; Randjelovic, D.; Markovic, B.; Papadimitriou, V.; Xenakis, A.; Lunter, D. J.; Zugic, A.; Savic, S. Microstructure and biopharmaceutical performances of curcumin-loaded low-energy nanoemulsions containing eucalyptol and pinene: Terpenes' role overcome penetration enhancement effect? *Eur. J. Pharm. Sci.* **2020**, *142*, No. 105135.

(7) Phillips, F. T. Effect of emulsifiers and organic diluents in soil insecticide and nematicide formulations. *Nature* **1959**, *184*, 1512−1513.

(8) Horner, J. L.; Truter, E. V. Emulsion reactions: the hydrolysis of wool wax. *Nature* **1950**, *165*, No. 771.

(9) Zembyla, M.; Murray, B. S.; Sarkar, A. Water-in-oil emulsions stabilized by surfactants, biopolymers and/or particles: a review. *Trends Food Sci. Technol.* **2020**, *104*, 49−59.

(10) Jiang, H.; Yang, H.; Ning, C.; Peng, L.; Zhang, S.; Chen, X.; Shi, H.; Wang, R.; Sarsenbekuly, B.; Kang, W. Amphiphilic polymer with ultra-high salt resistance and emulsification for enhanced oil recovery in heavy oil cold recovery production. *Geoenergy Sci. Eng.* **2025**, *252*, No. 213920.

(11) Yang, H.-B.; Jiang, H.; Xu, Z.; Zhang, X.; Wang, T.; Liu, H.; Ma, X.; Zhu, J.; Zhang, X.; Kang, W. Development and evaluation of organic/metal ion double crosslinking polymer gel for anti-CO_2 gas channeling in high temperature and low permeability reservoirs. *Pet. Sci.* **2025**, *22*, 725−738.

(12) Narayan, S.; Metaxas, A. E.; Bachnak, R.; Neumiller, T.; Dutcher, C. S. Zooming in on the role of surfactants in droplet coalescence at the macroscale and microscale. *Curr. Opin. Colloid Interface Sci.* **2020**, *50*, No. 101385.

(13) Saberi, A. H.; Fang, Y.; McClements, D. J. Fabrication of vitamin E-enriched nanoemulsions: Factors affecting particle size using spontaneous emulsification. *J. Colloid Interface Sci.* **2013**, *391*, 95−102.

(14) Jiang, W.; Xiang, W.; Xu, L.; Yuan, D.; Gao, Z.; Hu, B.; Li, Y.; Wu, Y. Fabrication, characterization, and emulsifying properties of hexadecyltrimethylammonium bromide (CTAB) complexed alginate microgel. *Food Hydrocolloids* **2023**, *140*, No. 108607.

(15) Hatchell, D.; Song, W.; Daigle, H. Effect of interparticle forces on the stability and droplet diameter of Pickering emulsions stabilized by PEG-coated silica nanoparticles. *J. Colloid Interface Sci.* **2022**, *626*, 824−835.

(16) Tian, J.; Chen, J.; Guo, J.; Zhu, W.; Khan, M. R.; Fu, Q.; Jin, Y.; Xiao, H.; Song, J.; Rojas, O. J. Pickering emulsions produced with kraft lignin colloids destabilized by in situ pH shift: Effect of emulsification energy input and stabilization mechanism. *Colloids Surf., A* **2023**, *670*, No. 131503.

(17) Kralchevsky, P. A.; Ivanov, I. B.; Ananthapadmanabhan, K. P.; Lips, A. On the thermodynamics of particle-stabilized emulsions: curvature effects and catastrophic phase inversion. *Langmuir* **2005**, *21*, 50−63.

(18) Zhao, Q.; Jiang, L.; Lian, Z.; Khoshdel, E.; Schumm, S.; Huang, J.; Zhang, Q. High internal phase water-in-oil emulsions stabilized by food-grade starch. *J. Colloid Interface Sci.* **2019**, *534*, 542−548.

(19) Pullanchery, S.; Kulik, S.; Rehl, B.; Hassanali, A.; Roke, S. Charge transfer across C−H···O hydrogen bonds stabilizes oil droplets in water. *Science* **2021**, *374*, 1366−1370.

(20) Beattie, J. K.; Djerdjev, A. M. The pristine oil/water interface: surfactant-free hydroxide-charged emulsions. *Angew. Chem., Int. Ed.* **2004**, *43*, 3568−3571.

(21) Golemanov, K.; Tcholakova, S.; Denkov, N. D.; Gurkov, T. Selection of surfactants for stable paraffin-in-water dispersions, undergoing solid−liquid transition of the dispersed particles. *Langmuir* **2006**, *22*, 3560−3569.

(22) Gharehkhani, S.; Ghavidel, N.; Fatehi, P. Kraft lignin-tannic acid as a green stabilizer for oil/water emulsion. *ACS Sustainable Chem. Eng.* **2019**, *7*, 2370−2379.

(23) Tao, S.; Jiang, H.; Gong, S.; Yin, S.; Li, Y.; Ngai, T. Pickering emulsions simultaneously stabilized by starch nanocrystals and zein nanoparticles: fabrication, characterization, and application. *Langmuir* **2021**, *37*, 8577−8584.

(24) Wang, S.; Yang, J.; Shao, G.; Qu, D.; Zhao, H.; Yang, L.; Zhu, L.; He, Y.; Liu, H.; Zhu, D. Soy protein isolated-soy hull polysaccharides stabilized O/W emulsion: Effect of polysaccharides concentration on the storage stability and interfacial rheological properties. *Food Hydrocolloids* **2020**, *101*, No. 105490.

(25) Miller, C.; Bageri, B. S.; Zeng, T. Z.; Patil, S.; Mohanty, K. K. Modified two-phase titration methods to quantify surfactant concentrations in chemical-enhanced oil recovery applications. *J. Surfactants Deterg.* **2020**, *23* (6), 1159−1167.
(26) Miqan, S. N.; Tabrizi, F. F.; Abedini, H.; Kashi, H. A. Estimation of micellization parameters of SDS in the presence of some electrolytes for emulsion polymerization systems. *J. Surfactants Deterg.* **2013**, *16* (2), 271−278.
(27) Freire, M. G.; Dias, A. M. A.; Coelho, M. A. Z.; Coutinho, J. A. P.; Marrucho, I. M. Aging mechanisms of perfluorocarbon emulsions using image analysis. *J. Colloid Interface Sci.* **2005**, *286*, 224−232.
(28) Dai, T.; Li, T.; Li, R.; Zhou, H.; Liu, C.; Chen, J.; McClements, D. J. Utilization of plant-based protein-polyphenol complexes to form and stabilize emulsions: Pea proteins and grape seed proanthocyanidins. *Food Chem* **2020**, *329*, No. 127219.
(29) Tong, Q.; Yi, Z.; Ma, L.; Tan, Y.; Chen, X.; Cao, X.; Liu, D.; Li, X. Polysaccharide-dependent depletion strategy to fabricate pickering emulsion gels. *Food Hydrocolloids* **2023**, *145*, No. 109175.
(30) Rehfeld, S. J. Stability of hydrocarbon-in-water emulsions during centrifugation. Influence of dispersed phase composition. *J. Colloid Interface Sci.* **1974**, *46* (3), 448−459.
(31) Jumaa, M.; Muller, B. W. Parenteral emulsions stabilized with a mixture of phospholipids and PEG-660−12-hydroxy-stearate: evaluation of accelerated and long-term stability. *Eur. J. Pharm. Biopharm.* **2002**, *54*, 207−212.
(32) Tao, S.; Guan, X.; Li, Y.; Jiang, H.; Gong, S.; Ngai, T. All-natural oil-in-water high internal phase Pickering emulsions featuring interfacial bilayer stabilization. *J. Colloid Interface Sci.* **2022**, *607*, 1491−1499.
(33) Gao, Z.; Gao, C.; Jiang, W.; Xu, L.; Hu, B.; Yao, X.; Li, Y.; Wu, Y. In situ crosslinking sodium alginate on oil-water interface to stabilize the O/W emulsions. *Food Hydrocolloids* **2023**, *135*, No. 108233.
(34) Marefati, A.; Matos, M.; Wiege, B.; Haase, N. U.; Rayner, M. Pickering emulsifiers based on hydrophobically modified small granular starches Part II - Effects of modification on emulsifying capacity. *Carbohydr. Polym.* **2018**, *201*, 416−424.
(35) Stokes, G. G. On the effect of the internal friction of fluids on the motion of pendulums. *Trans. Cambridge Philos. Soc.* **1851**, *9* (8), 8−106.

https://doi.org/10.1021/acs.langmuir.5c01936
Langmuir 2025, 41, 14570−14578